

T. PIECZONKA*, M. SUŁOWSKI*, A. CIAŚ*

ATMOSPHERE EFFECT ON SINTERING BEHAVIOUR OF ASTALOY CrM AND ASTALOY CrL HÖGANÄS POWDERS WITH MANGANESE AND CARBON ADDITIONS

WPLYW ATMOSFERY NA SPIEKALNOŚĆ KOMERCYJNYCH PROSZKÓW HÖGANÄS ASTALOY CrM I ASTALOY CrL Z DODATKAMI MANGANU I WĘGLA

Dilatometric data for Astaloy CrM (3% Cr-0.5% Mo) and Astaloy CrL (1.5% Cr-0.2% Mo) powders with additions of 0.3% carbon and 3.0% manganese during sintering cycles up to 1120 and 1250°C in different atmospheres are reported. For comparison, also Astaloy CrM and Astaloy CrL powders were investigated. Starting with green densities of approx. 6.8 g/cm³, the final density of sintered compacts was influenced mainly by the sintering temperature, while the results showed the only minor effect of the sintering atmosphere on the final dimensional changes. However, the sintering atmosphere influences the sintering behaviour, microstructure and the final chemical composition of sintered compacts. In sintered and in the dilatometer cooled Mn-Cr-Mo-C steels predominantly bainitic structures were obtained.

Keywords: pre-alloyed iron based powders, sintering, dimensional control, dilatometry

Praca przedstawia wyniki badań dylatometrycznych procesu spiekania mieszanek proszków zawierających, jako podstawowe, proszki Astaloy CrM (3% Cr-0.5% Mo) i Astaloy CrL (1.5% Cr-0.2% Mo) oraz dodatki 3% mas. Mn i 0.3% mas. C. Spiekanie izotermiczne realizowane było w dwóch temperaturach: 1120°C i 1250°C, a atmosferami spiekania były gazy: azot, mieszanina 95% obj. azotu + 5% obj. wodoru i argon. Gęstość spieków determinowana jest głównie temperaturą spiekania, a wpływ atmosfery jest nieznaczny. Jednakże od rodzaju atmosfery spiekania uzależnione jest zachowanie się materiałów w trakcie cykli termicznych, jakim są poddane podczas spiekania. Atmosfera spiekania ma również wpływ na mikrostrukturę spieków oraz na zmiany składu chemicznego towarzyszące spiekaniu. Głównym składnikiem struktury spieków uzyskanej bezpośrednio po spiekaniu w warunkach chłodzenia dostępnych w dylatometrze był bainit.

1. Introduction

Chromium and manganese are potentially important alloying elements in sintered steels. When correctly employed, they can improve mechanical properties, hardenability and nitridability [1-6]. For these reasons Cr and Mn are the elements, which are widely used in many structural wrought steels. However, up to date, these elements have seen little exploitation in the powder metallurgy (PM) industry due to their extremely high affinity for oxygen [7-16]. One of the recent (1998) industrially available means of incorporating chromium into structural PM parts production is use of the water atomised pre-alloyed Astaloy CrM (Fe-3%Cr-0.5%Mo) powder developed by Höganäs AB [17]. This producer delivers also (since 2002) a modified powder grade Astaloy CrL (Fe-1.5%Cr-0.2%Mo) [18]. Sintered compacts made of these powders alloyed with carbon indicate attractive

mechanical properties, including sinterhardening effect [19-28]. The limited use of both powders in PM industry is associated with the processing requirements of very low dew point/oxygen potential of the sintering atmosphere at normal link-belt sintering temperatures. The atmosphere requirements are relaxed by the use of elevated sintering temperatures (above 1200°C) [1]. There has been, however, a reluctance on the part of manufacturers to use this technique in, for example, walking beam or pusher furnaces on the grounds of cost and availability. This situation is changing with the introduction of modern, more cost efficient furnaces.

Because high temperature sintering (HTS) promotes oxide reduction, it is especially very useful PM route for steels containing elements which have a high affinity for oxygen, particularly if they are added in elemental form. HTS further promotes homogenisation of the microstructure and pore rounding, which can lead to the improve-

* AGH UNIVERSITY OF SCIENCE AND TECHNOLOGY, FACULTY OF METALS ENGINEERING AND INDUSTRIAL COMPUTER SCIENCE, 30-059 KRAKÓW, 30 MICKIEWICZA AV., POLAND

ment in the mechanical properties of PM steels [4]. Additionally, the hardenability of Astaloy CrM and Astaloy CrL steels can be further increased by manganese addition to the starting powder, and e.g. Mitchell et al [1-4] have reported or obtaining martensite, including by air hardening, and presented initial sinterhardening data.

It is well known in PM industry that the dimensional changes occurring during the whole PM cycle have to be carefully controlled to produce high precise parts and to keep required tolerances. There are many parameters influencing the dimensional behaviour of the compact during sintering. Main of them is the sinterability of the material subjected to the specific external conditions, which includes chemical homogenisation and material – sintering atmosphere interactions. Thus, in this paper a study of the temperature and atmosphere effect on dimensional changes of Mn and C containing compacts based on Astaloy CrM and Astaloy CrL Höganäs grade powders is shown.

2. Experimental procedure

The following starting powders were used:

- commercial pre-alloyed Fe-3% Cr-0.5% Mo Höganäs Astaloy CrM grade powder,
- commercial pre-alloyed Fe-1.5% Cr-0.2% Mo Höganäs Astaloy CrL grade powder,
- smaller than 40 μm fraction (distribution centred around 10 μm) of low carbon Elkem ferromanganese powder supplied by Elkem Ferromanganese Sauda, Norway, containing 77.0 mass% Mn, 1.3 mass% C, 0.2 mass% O₂, 0.02 mass% N₂ and Fe – bal.,
- commercial C-UF Höganäs fine graphite powder.

The lubricant was not added.

The starting powders were mixed in Turbula mixer for 30 minutes to prepare the following mixtures:

- Astaloy CrM + 0.30 mass% C + 3.0 mass% Mn,
- Astaloy CrL + 0.30 mass% C + 3.0 mass% Mn,

For comparison, the compacts based on as-received Astaloy CrM and Astaloy CrL powders were also used.

Mixtures were carefully handled to minimise any segregation of the constituents. The mixtures were compacted into rectangular specimens of size 4×4×15 mm³, using uniaxial pressing at 600 MPa. This resulted in green densities of about 6.8 g/cm³. The sintering experiments were carried out in a horizontal push rod dilatometer NETZSCH 402E. The measuring direction (length of the specimen) was chosen perpendicular to the pressing direction of the compacts.

The gases used as the sintering atmospheres were:

- nitrogen, purity 5.0
- 95 vol.% nitrogen + 5 vol.% hydrogen mixture prepared from 5.0 purity gases, and

- argon, purity 4.5.

The dew point measured at the inlet to the dilatometer was at least –55°C. The flow rate was 50 ml/min at the internal tube diameter of 38 mm.

Samples were heated at 10°C/min to the isothermal sintering temperature of either 1120°C or 1250°C. Isothermal sintering was then carried out for 60 minutes. It should be noted that the dilatometer used could not maintain the constant cooling rate during the whole cooling period. Thus, the cooling rate within the linear range (from isothermal temperature down to about 380°C) was 20°C/min (0.33°C/s). Below 380°C, the cooling rate was decreasing continuously as it is seen on T-curves (e.g. in Figure 1). The temperature control was accurate to $\pm 1^\circ\text{C}$. The changes in slope of the dilatometric traces were examined in detail (Figures 5-7).

Sintered compacts were used to prepare metallographic specimens by 2% nital etching. The microstructures of sintered compacts were observed by light microscopy.

3. Results and discussion

Figures 1-4 show the complete dilatometric plots obtained during the current investigations. In the case of unmodified Astaloy CrL and Astaloy CrM powders, used as standard materials, initially the thermal expansion is observed, then the shrinkage due to $\alpha \rightarrow \gamma$ transformation begun at $\sim 888^\circ\text{C}$ and $\sim 878^\circ\text{C}$, respectively, and finished at $\sim 918^\circ\text{C}$ for both powders, being $\sim 0.20\%$ with minor effect of the atmosphere. The isothermal dimensional changes of pure Astaloy CrL and Astaloy CrM compacts are strongly influenced by the temperature. During sintering at 1120°C, the changes are negligible, irrespective of the sintering atmosphere, while at 1250°C the effect of the sintering atmosphere is significant: the $\sim 0.45\%$ shrinkage is observed for both powders but only in hydrogen containing atmosphere (95% N₂/5 %H₂). This behaviour can be explained by the extending oxides reduction at higher temperature [22]. Cooling period is characterised by the $\gamma \rightarrow \alpha$ transformation starting earlier (i.e. at higher temperature) in argon than in other atmospheres. Astaloy CrL specimens cooled from 1120°C began to expand due to the transformation at $\sim 870^\circ\text{C}$ in argon and at $\sim 850^\circ\text{C}$ in nitrogen and nitrogen/hydrogen mixture. In case of Astaloy CrM the respective temperatures are: $\sim 880^\circ\text{C}$ and $\sim 830^\circ\text{C}$. Compacts cooled after sintering at 1250°C start to transform at $\sim 880^\circ\text{C}$ in argon (irrespective of the powder grade) while at $\sim 840^\circ\text{C}$ for Astaloy CrL and only at $\sim 820^\circ\text{C}$ for Astaloy CrM in other atmospheres.

Specimens containing manganese and graphite heated from room temperature initially expand thermally, till

~680°C in argon atmosphere and till the beginning of $\alpha \rightarrow \gamma$ transformation in other atmospheres, which are: ~780°C for Astaloy CrL-base composition and ~815°C for Astaloy CrM-base one. Similarly to the not modified powders, the dimensional behaviour of Mn and C alloyed mixtures in argon differs from those in nitrogen and nitrogen/hydrogen mixture. The expansion rate starts to decrease slightly only in argon at by ~130°C (Astaloy CrL base powder) or even by ~160°C (Astaloy CrM) lower temperature than that of the initiation of the $\alpha \rightarrow \gamma$ transformation, which is better visible in

Figure 5. Generally, Mn and C lower the temperature at which this transformation starts. This is important since it has been demonstrated by Mitchell et al [1, 4] that alpha phase sintering in Astaloy CrM-base alloys is to be avoided. Except argon, there were only minor effects due to the composition of the sintering atmosphere on the $\alpha \rightarrow \gamma$ transformation. It is, however, worthy of note that the thermal conductivity of the sintering atmosphere was anticipated to be of more importance during cooling, especially when sinter hardening effects were expected.

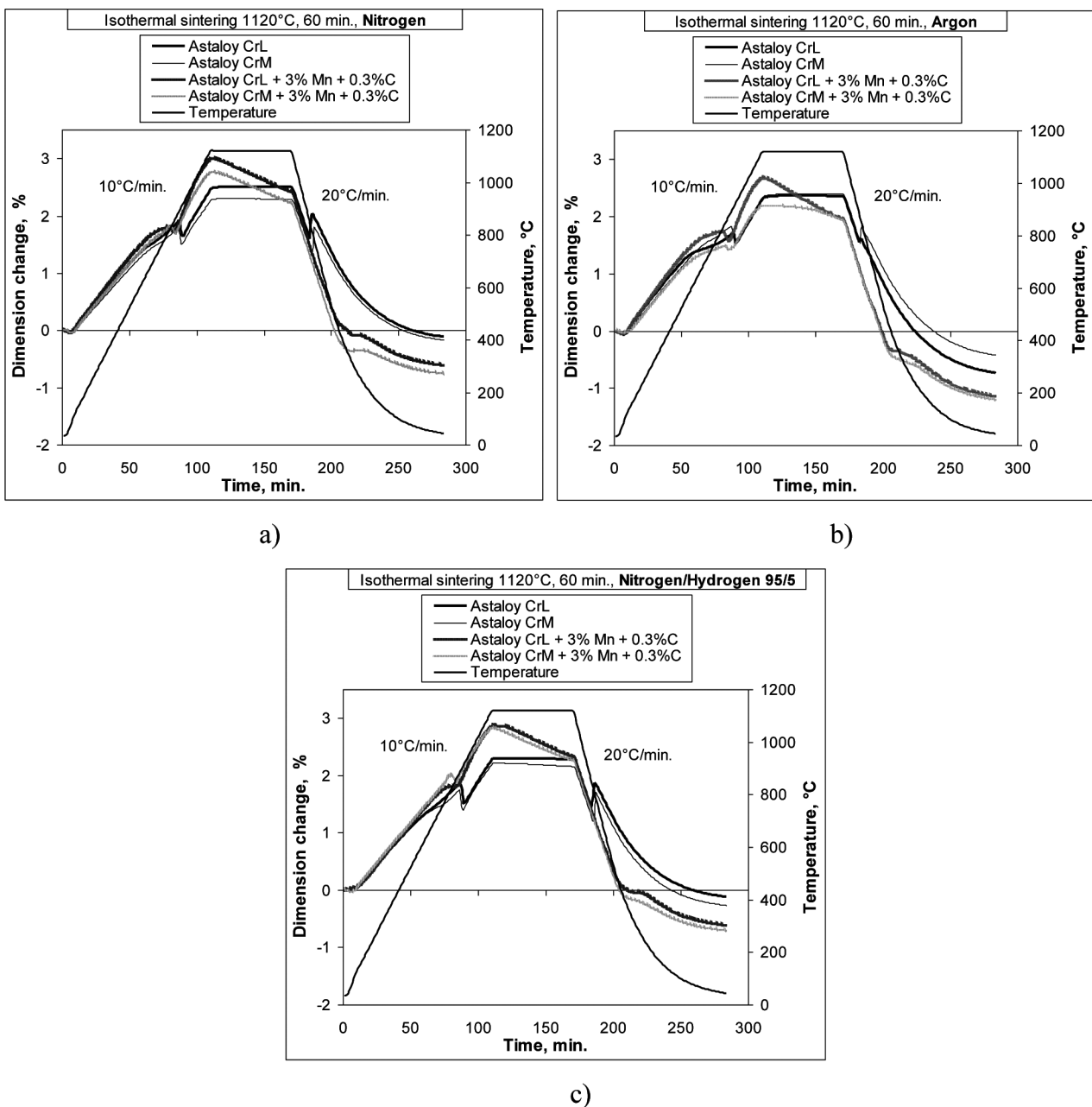


Fig. 1. Dilatometric curves for sintering cycles at 1120°C under different furnace atmospheres: a) nitrogen, b) argon, c) nitrogen/hydrogen 95/5. The details are given in individual figures

After completion of the $\alpha \rightarrow \gamma$ transformation the specimens expand until the sintering plateau, due to thermal expansion and possibly also alloying and other sintering processes. The slopes of the dilatometric curves in this increasing temperature region depend on composition of the mixtures, being steeper for those based on Astaloy CrL powder, implying that homogenisation processes continue to take place. All the specimens sintered at 1120°C expanded continuously during heating at almost constant rate, independently of the atmosphere (Fig. 1), whereas those heated to 1250°C reached their maximal length admittedly at that temperature, but start-

ing at about 1200°C at significantly lower expansion rate, which indicates that sintering shrinkage begins to dominate thermal expansion, starting just at 1200°C (Fig. 2).

There was observed only a minor effect of the sintering atmosphere on isothermal shrinkage. At 1120°C (Fig. 1) both mixtures shrank by ~0.6%, while at 1250°C (Fig. 2) by ~1.3% in case of Astaloy CrL based composition and by ~1.4% for Astaloy CrM based one.

The influence of sintering atmosphere on dimensional changes is more clearly illustrated in Figs 3 and 4. Interestingly, the argon produces the highest final shrinkage.

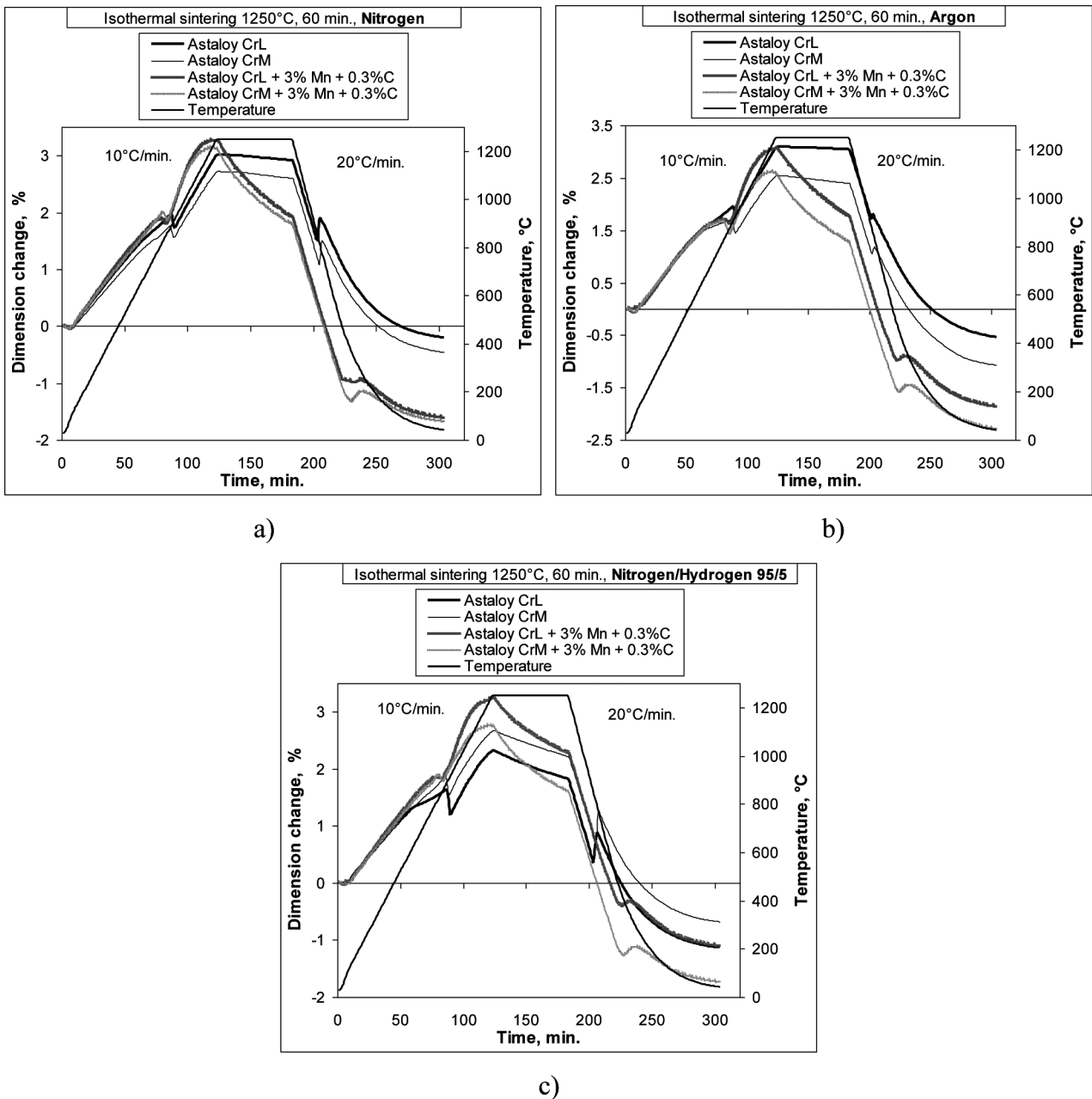


Fig. 2. Dilatometric curves for sintering cycles at 1250°C under different furnace atmospheres: a) nitrogen, b) argon, c) nitrogen/hydrogen 95/5. The details are given in individual figures

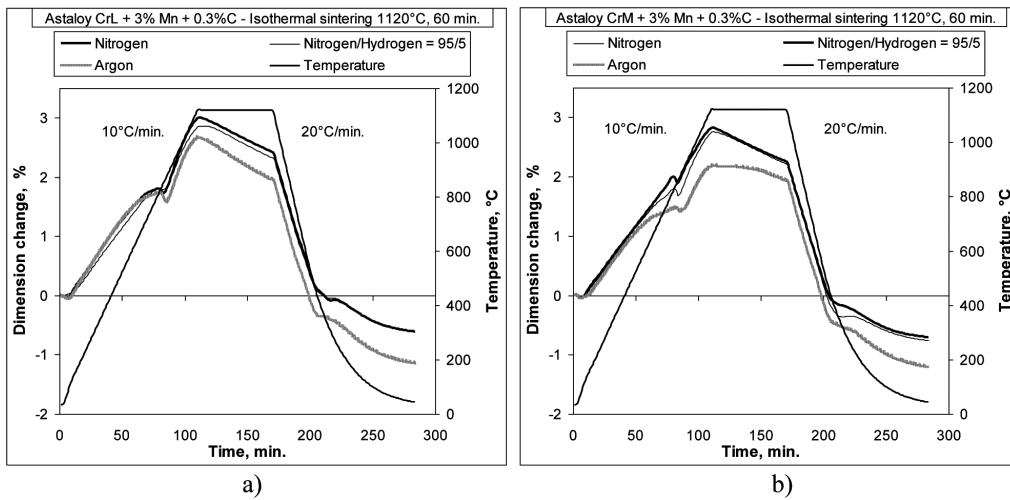


Fig. 3. The influence of the sintering atmosphere on dimensional changes for specimens sintered at 1120°C: a) based on Astaloy CrL powder, b) based on Astaloy CrM powder

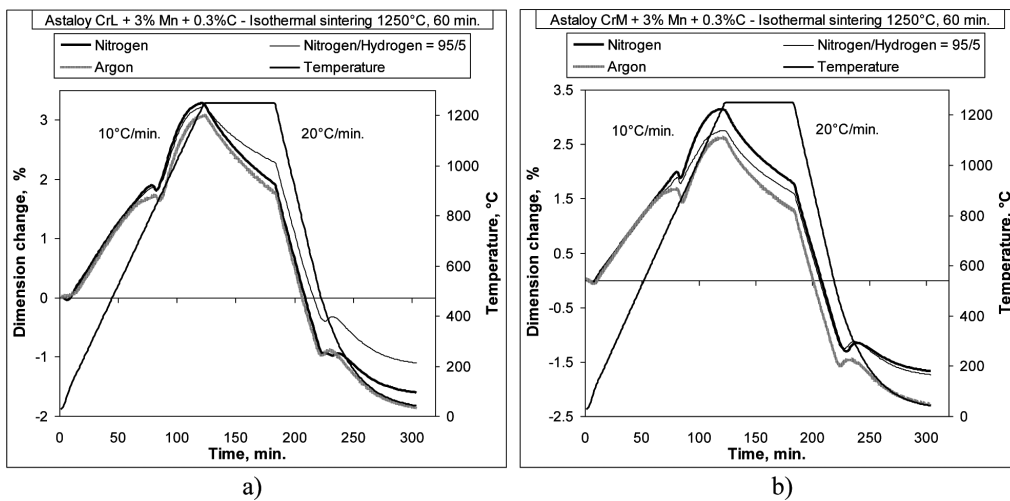


Fig. 4. The influence of the sintering atmosphere on dimensional changes for specimens sintered at 1250°C: a) based on Astaloy CrL powder, b) based on Astaloy CrM powder

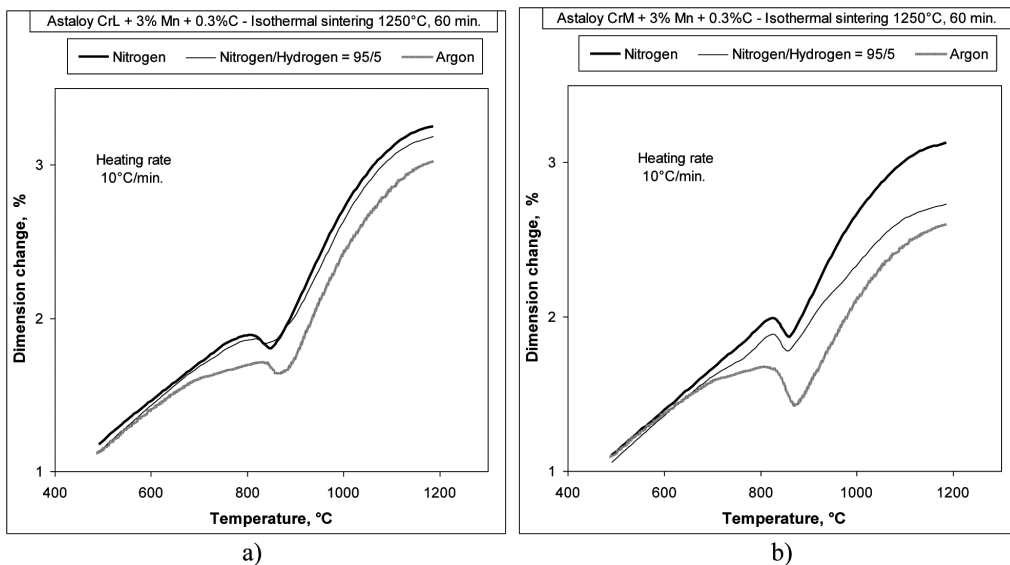


Fig. 5. Detailed dilatometric heating segments: a) for steel based on Astaloy CrL powder, b) for steel based on Astaloy CrM powder

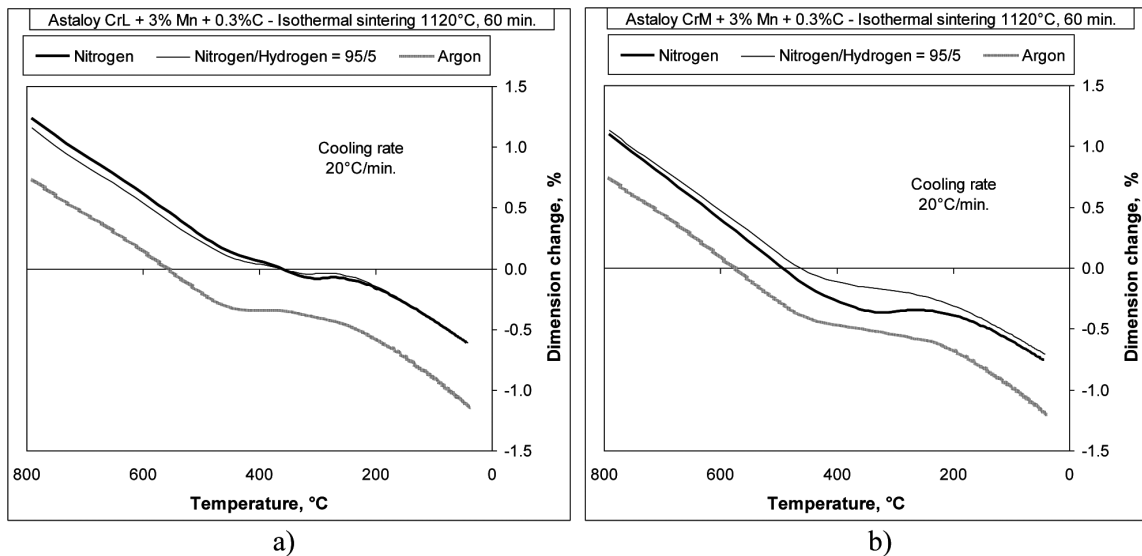


Fig. 6. Detailed dilatometric cooling segments for compacts sintered at 1120°C: a) for steel based on Astaloy CrL powder, b) for steel based on Astaloy CrM powder

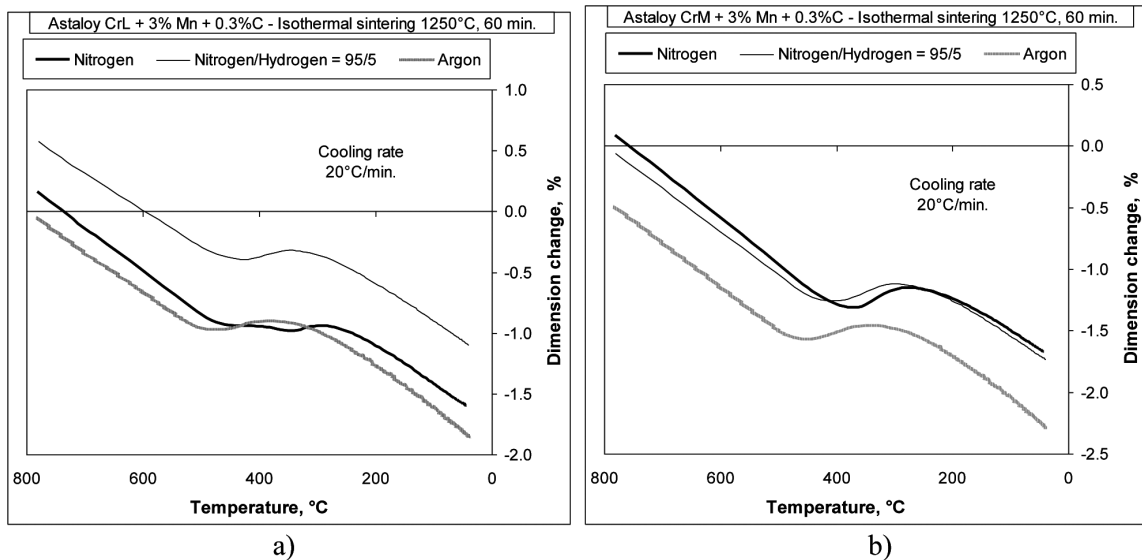


Fig. 7. Detailed dilatometric cooling segments for compacts sintered at 1250°C: a) for steel based on Astaloy CrL powder, b) for steel based on Astaloy CrM powder

The addition of carbon and ferromanganese to the Astaloy CrL and Astaloy CrM powders, which enhances sinter hardening effects, can be related to the cooling segments of the dilatometric curves (Figs 6 and 7). In the contrary to the unmodified base powders, the $\gamma \rightarrow \alpha$ transformation is not detected now. Because of the advanced homogenisation, the sintered alloys show increased hardenability. Thus the approximate bainite start temperatures appear to be $\sim 470^\circ\text{C}$ for Astaloy CrL + 0.3% C + 3% Mn and $\sim 460^\circ\text{C}$ for Astaloy CrM + 0.3% C + 3% Mn, respectively for compacts sintered at 1120°C. The sintering temperature of 1250°C increases the bainite start temperature (B_s) by about 40°C, which

accords with previous results [29]. Independently of the composition and isothermal sintering temperature, B_s temperature is by about 20°C higher in argon than in other atmospheres.

The higher heat conductivity of the 95% N_2 /5% H_2 atmosphere during cooling made only a negligible difference in heat transfer when the non-linear region of cooling rate was reached, probably due to the small thermal mass of the dilatometric sample. Thus sinter hardening was not significantly influenced by the high heat conductive hydrogen.

It is well known in PM steel that carbon not only changes the transformations behaviour but also acts as a

reducing agent. The last role is connected with some loss of this element during sintering. Sintered compacts produced in dilatometer were subjected to LECO analysis to control the effect of sintering conditions on expected decarburising and nitriding. Additionally, the oxygen content was also measured. The results are collected in Table 1.

It can be seen from Table 1 that the influence of the atmosphere on changes of the chemical composition is more pronounced for higher sintering temperature. However, for all experimental conditions the carbon content substantially decreases which is related to the oxides reduction and reactions with residual impurities of the sintering atmosphere. Surprisingly, the gas mixture 95 vol.% nitrogen + 5 vol.-% hydrogen seems to be a strong decarburising and simultaneously oxidising environment at 1250°C, which was observed for both materials. The loss of carbon in those compacts is associated with its oxidation. In turn, the increased oxygen content can be

explained by the oxidising effect of the water vapour during cooling. The atmospheres containing nitrogen cause slight nitriding of both steels, however the material based on Astaloy CrM is more sensitive for nitriding. The results showed the large decrease of carbon concentration: from ~25% up to ~75% as compared with that in green compacts. At higher sintering temperatures the higher carbon reduction was recorded.

Thermodynamics indicates favourable conditions for carbothermic reduction of Cr and Mn oxides at conventional sintering temperatures. The possible reactions were described in [30]. For reduction of Cr_2O_3 and MnO by solid carbon thermodynamic calculations for atmosphere predominantly of nitrogen were carried out by Cias and Mitchell [24, 31]. Comparison of calculated ratio of partial pressures $p(\text{CO})/p(\text{CO}_2)$ and maximum allowed partial pressure of O_2 and H_2O in the 90% $\text{N}_2/10\% \text{H}_2$ atmosphere with the experimentally obtained one, by continuous atmosphere monitoring during

TABLE 1

LECO analysis of compacts sintered in different atmospheres

Material (powder used), mass%	Sintering atmosphere	Sintering temperature, °C					
		1120			1250		
		mass. %			mass. %		
		Carbon	Oxygen	Nitrogen	Carbon	Oxygen	Nitrogen
Astaloy CrL + 3Mn+ 0.3C	Nitrogen	0.17	0.16	0.08	0.11	0.04	0.08
	95% $\text{N}_2/5\% \text{H}_2$	0.14	0.14	0.08	0.06	0.19	0.07
	Argon	0.22	0.12	0.00	0.12	0.07	0.00
Astaloy CrM + 3Mn+ 0.3C	Nitrogen	0.16	0.14	0.11	0.11	0.04	0.12
	95% $\text{N}_2/5\% \text{H}_2$	0.15	0.16	0.13	0.05	0.12	0.13
	Argon	0.15	0.13	0.00	0.17	0.02	0.00

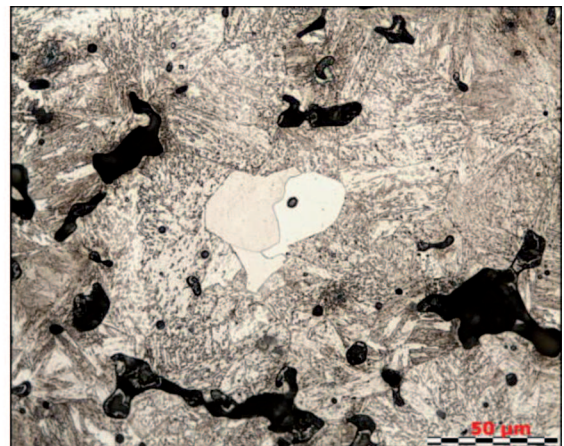
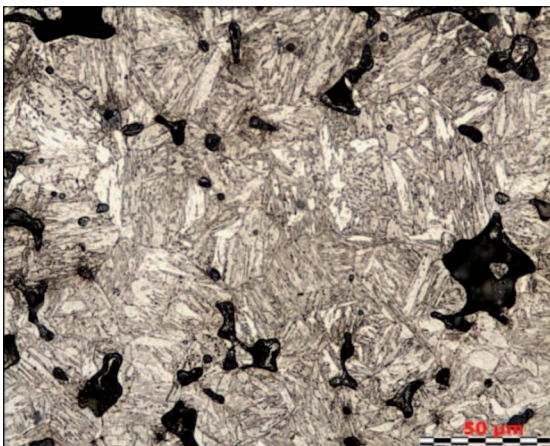


Fig. 8. Microstructure of Astaloy CrL + 0.3 wt% C + 3 wt% Mn sintered at 1250°C: left – in $\text{N}_2/\text{H}_2 = 95/5$, right – in argon

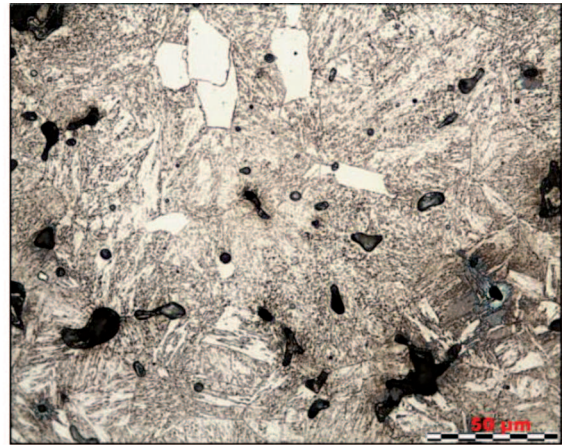
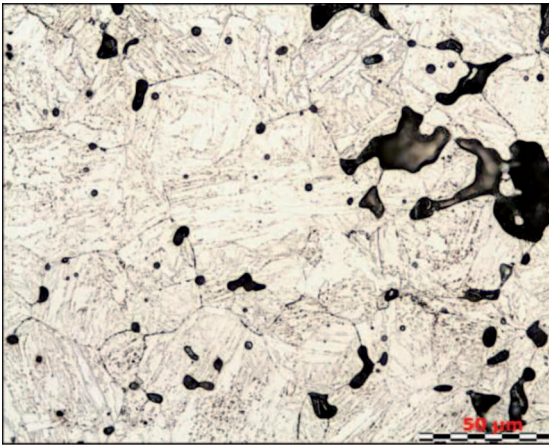


Fig. 9. Microstructure of Astaloy CrM + 0.3 wt% C + 3 wt% Mn sintered at 1250°C: left – in $N_2/H_2 = 95/5$, right – in argon

the sintering of Astaloy CrM + 0.5% C, clearly shows favourable conditions for carbothermic reduction of the chromium oxides during isothermal sintering at 1120°C or higher [32]. The effect of the sintering atmosphere is not unambiguous. The relatively low carbon concentration in sintered steels seems to be responsible for their rather limited sinterhardenability. The examples of sintered microstructures are shown in Figures 8 and 9.

Generally for both base powders, sintering in nitrogen and in 95% $N_2/5\%$ H_2 gas mixture produces homogeneous bainitic microstructure with rounded pores, whereas the microstructure of compacts sintered in argon is characterised by bainitic matrix containing one phase bright grains. The identification of the phase and the role of argon in its appearance require further investigations.

4. Conclusion remarks

The relatively small shrinkages observed at the sintering temperatures probably resulted from solid state sintering of the compacts with a relatively low green density of approx. 6.8 g/cm^3 . In accordance with the theoretical phase diagrams, for the Fe-3%Cr-0.5%Mo-C and Fe-1%Cr-3%Mn-0.5%Mo-C systems [33], to obtain a liquid phase for the alloys investigated temperatures of the order of 1400°C are required. Therefore to increase densification at chosen isothermal temperatures this sintering period should be elongated. Based on isothermal shrinkage rate shown in Figures 1 and 2 it can be stated that there is still a potential for further shrinkage at these temperatures.

The influence of the sintering atmosphere on changes of the chemical composition is more visible for higher sintering temperature. The gas mixture in amount of 95 vol.-% N_2 + 5 vol.-% H_2 seems to be a strong decarburising agent and also oxidising environment at 1250°C, which was observed for both materials. The

loss of carbon in investigated compacts is associated with its oxidation. The increase of oxygen content can be explained by the oxidising effect of the water vapour during cooling.

Why argon modifies the sintering behaviour and microstructure of materials investigated is not completely clear. Probably it can be explained, at least partly, by the low heat conductivity of this gas. The further investigations in this field, including mechanical properties of in argon sintered compacts, are under way.

Acknowledgements

This paper was presented during 6th International Conference on Powder Metallurgy which was held in Ankara, 6-9 October 2011. The financial support of the Ministry of Science and Higher Education under the contract no N N507 477237 (AGH no 18.18.110.961) is gratefully acknowledged.

REFERENCES

- [1] S.C. Mitchell, A.S. Wronski, A. Cias, M. Stoytchev, Proc. PM²TEC'99, MPIF, Princeton, New Jersey 2, Part 7 – P/M steels, 129 (1999).
- [2] A.S. Wronski, B.S. Becker, C.S. Wright, S.C. Mitchell, Proc. DFPM'99, ed. L. Parilak and H. Danninger 1, 155 (1999).
- [3] S.C. Mitchell, The Development of Powder Metallurgy Manganese Containing Low-Alloy Steels (Ph.D. thesis, University of Bradford, Bradford, 2000, in English).
- [4] A.S. Wronski, A. Cias, P. Barczy, M. Stoytchev et al, Tough Fatigue and Wear Resistant Sintered Gear Wheels, Final Report on EU Copernicus Contract No. ERB CIPA CT-94-0108, European Commission 1998.
- [5] B. Lindley, B. James, Proc. Advances in Powder Metallurgy & Particulate Materials, MPIF, Hollywood 10, 36 (2010).

- [6] E. Hryha, E. Dudrova, L. Nyborg, Metallurgical and Materials Transactions A-Physical Metallurgy and Materials Science **41A** (11), 2880.
- [7] E. Navara, Proc. Sintering'85, compiled by G.C. Kuczynski et al., Plenum Press, 343 (1985).
- [8] A.N. Klein, R. Oberacker, F. Thümmel, Powder Metallurgy International **17**, 1, 13 (1985).
- [9] A.N. Klein, R. Oberacker, F. Thümmel, Powder Metallurgy International **17**, 2, 71 (1985).
- [10] A. Salak, Powder Metallurgy International **16**, 6, 260 (1984).
- [11] A. Salak, International Journal of Powder Metallurgy **16**, 4, 369 (1980).
- [12] H. Danninger, R. Pöttschacher, G. Jang, J. Seyrkammer, A. Salak, Proc. PM'94 World Congress, EPMA, Paris **1**, 879 (1994).
- [13] H. Danninger, C. Gierl, Science of Sintering **40**, 33 (2008).
- [14] M. Selecka, A. Salak, T. Pieczonka, M. Stoytchev, Proc. EURO PM2007, EPMA **1**, 47 (2007).
- [15] M. Selecka, A. Salak, T. Pieczonka, Steel Grips **6**, 5, 355 (2008).
- [16] E. Hryha, L. Nyborg, E. Dudrova, S. Bengtsson, Proc. EURO PM2009 (CD) EPMA, Copenhagen, Denmark 2009.
- [17] C. Lindberg, Proc. Advances in Powder Metallurgy and Particulate Materials, MPIF **2**, 7-229 (1999).
- [18] U. Engstrom, A. Klekovkin, S. Berg, B. Edwards, L. Frayman, G. Hinzmann, D. Whitehouse, Proc. Advances in Powder Metallurgy & Particulate Materials, MPIF, Las Vegas, USA **7**, 68 (2003).
- [19] A. Molinari, G. Straffelini, P. Campestrini, Powder Metallurgy **42**, 3, 235 (1999).
- [20] U. Engström, Proc. Advances in Powder Metallurgy & Particulate Materials, MPIF **5**, 5-147 (2000).
- [21] C. Lindberg, B. Johansson, B. Maroli, Proc. Advances in Powder Metallurgy & Particulate Materials, MPIF **6**, 6-81 (2000).
- [22] F. Castro, P. Ortiz, Proc. of EURO PM2003, Valencia, Spain **1**, 243 (2003).
- [23] O. Bergman, L. Nyborg, Powder Metallurgy Progress **10**, 1, 1 (2010).
- [24] A. Ciał, Development and Properties of Fe-Mn-(Mo)-(Cr)-C Sintered Structural Steels (AGH-UST, Uczelniane Wydawnictwo Naukowo-Dydaktyczne, Kraków 2004).
- [25] M. Sułowski, Archives of Metallurgy and Materials **52**, 4, 617 (2007).
- [26] M. Sułowski, K. Faryj, Archives of Metallurgy and Materials **54**, 1, 121 (2009).
- [27] A. Ciał, M. Sułowski, Archives of Metallurgy and Materials **54**, 4, 1093 (2009).
- [28] M. Sułowski, A. Ciał, Archives of Metallurgy and Materials **56**, 2, 293 (2011).
- [29] M. Sułowski, Powder Metallurgy Progress **8**, 2, 151 (2008).
- [30] A. Ciał, S.C. Mitchell, K. Pilch, H. Ciał, M. Sułowski, A.S. Wronski, Powder Metallurgy **46**, 2, 165 (2003).
- [31] S.C. Mitchell, A. Ciał, Powder Metallurgy Progress **4**, 3, 132 (2004).
- [32] E. Hryha, E. Čajkova, E. Dudrová, Powder Metallurgy Progress **7**, 4, 181 (2007).
- [33] T. Pieczonka, S.C. Mitchell, M. Stoytchev, M. Kowalczyk, Proc. of the 2002 Int. Conf. on Powder Metallurgy & Particulate Materials, Orlando, USA **11**, 14 (2002).